

# High Speed Camera Observation of Electrospray

Hyun-Ha Kim, Atsuchi Ogata, and Jong-Ho Kim,

**Abstract**—A high speed camera was implemented to visualize the detailed structure of electrospray. Applied voltage to the nozzle was found to be a primary factor determining the spray mode. The spray modes observed in the electrospray of deionized water include dripping mode, dripping with jet, spindle mode and cone-jet mode. The cone-jet mode also subdivided into oscillating cone-jet, rotating cone-jet, stable cone-jet, and unstable cone-jet. The size of nozzle also influenced the voltage range for each spray mode. The size of droplet was mostly determined by the spray pattern releasing the droplets; fine jet > cone-jet > break-up of cone-jet. The voltage range for the stable cone-jet mode became wide as the nozzle diameter increased.

**Index Terms**—Electrospray, High Speed Camera, Corona Discharge, Spray Mode, Cone-Jet, Charged Droplet

## I. INTRODUCTION

ELECTROSPRAY has been used in various applications such as generation of highly dispersed micro- and nanoparticles, ink-jet printing, paint spraying, fuel atomization, ion sources in mass spectrometer, agricultural treatment, surface coating etc. Electrospray provides a simple way to obtain fine microdroplets of various liquids [1]. The mechanism of electrospray has been the subject of extensive researches during the late century. The early works may date back to Rayleigh in 1880s and Zeleny from late 1890 to 1920s [2-4]. There have been a great numbers of publications reporting both scientific studies and practical applications [5].

Fine droplet formation in an electrospray process is often explained by the hydrostatic balance between two key factors of electrostatic force and surface tension. Lord Rayleigh first tried a theoretical analysis of the break-up of liquid under electrical stress and derived instability condition for the electrically charged droplets. His theory is based on the balance between the repulsive electrostatic force and the surface tension of the liquid restoring forces. Rayleigh limit for the instability of charged droplet is given by

$$Q = (8\pi^2 \epsilon_0 \gamma d^3)^{1/2} \quad (1)$$

Where  $Q$  is the charge on the droplet,  $\epsilon_0$  the permittivity of the

surrounding gas,  $\gamma$  the surface tension of the liquid and  $d$  is the diameter of droplet. When the electrostatic force overcomes the surface tension of the liquid interest, electrically charged fine droplets are ejected from cone [6]. It is also referred to as Coulomb fission [7]. This relationship has been evaluated by a number of charge-to-mass ratio measurements [8-10], and size distribution [10-12]. However, the real process is greatly influenced by many parameters and these two forces can not explain all the phenomena encountered in the electrospray. Michelson indicated that the Rayleigh's analysis considering only the electrical stress and surface tension is oversimplified [13]. Classification of spray mode has also been the subject of intensive works, which can provide insight into the electrospray [14-16]. The size of liquid droplets ejected for an electrospray varies from the millimeter to the submicron range.

According to the published literature, the parameters investigated in the electrospray process include the type of liquid, conductivity, nozzle diameter, applied voltage and its polarity, liquid volume flow rate and so on. The understanding of detailed feature of the electrospray is particular important, because the size and concentration control offer a wide spectrum of practical applications.

In this work, a high speed camera was implemented to visualize the detailed time-resolved structure of electrospray. The changes of spray mode were studied with increasing the applied voltage to the spray nozzle. We also present the influence of nozzle diameter on the spray mode.

## II. EXPERIMENTAL

### A. Electrospray setup

Experimental setup is illustrated in Figure 1. Plastic syringe with stainless steel needle was used, where the needle exerted as high voltage electrode. Three nozzles with different inner diameters (0.2 mm, 0.3 mm and 0.4 mm) were used in this study. The gap between the tip of the needle and the ground plate was 3 cm. There was no forced liquid flow and the water fell down only by gravity. Electrical conductivities were measured with a conductivity meter (Mettler Toledo). The used deionized water and tap water had electrical conductivities of 3.3  $\mu\text{S}/\text{cm}$  and 300  $\mu\text{S}/\text{cm}$ , respectively. Digital oscilloscope (Tektronix, Model TDS 3034B) was used to measure the applied voltage. High voltage probes (Tektronix, Model 6101A) were used to monitor the voltages applied to the spray nozzle. The current in the electrospray was measured using a Keithley electrometer (Model 6514).

Hyun-Ha Kim is with the National Institute of Advanced Industrial Science and Technology (AIST) Tsukuba, Ibaraki 305-8569 Japan (corresponding author to provide phone: +81-29-861-8061; fax: +81-29-861-8866; e-mail: hyun-ha.kim@aist.go.jp).

Atsushi Ogata is with the National Institute of Advanced Industrial Science and Technology (AIST) Tsukuba, Ibaraki 305-8569 Japan (e-mail: atsushi-ogata@aist.go.jp).

Jong-Ho Kim is with, the Department of Environmental Engineering, HanSeo University, Korea (e-mail: kimjh@hanseo.ac.kr)

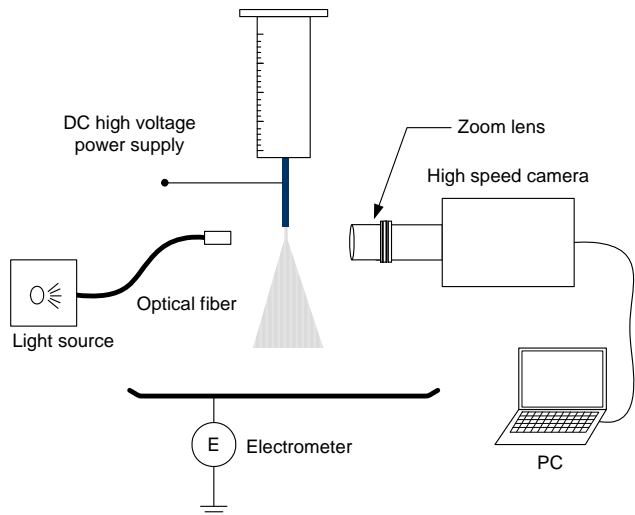


Fig.1 Experimental setup.

### B. High Speed Camera Setup

A high speed digital camera (Photron Co.; FASTCAM-SA1.1 Model 675K-M2), capable of 1000000 frames per second (fps) at maximum, was used to get visual images of the electro spray. A zoom lens (Leica, Model Z6 APO) was attached to the high speed camera to get enlarged images near the spray nozzle. A continuous light source (Sumita Co, Model MS-M180) was set at the opposite position of the camera. Light was focused the tip of the needle with an optical fiber, which enables to get clear image even at short exposure time of the camera. The shadow images of the droplets were recorded by the high speed camera at 100  $\mu$ s intervals (10000 fps). The camera gate time for each snap shot was 1  $\mu$ s. The resolution of the image was  $512 \times 1024$  pixels. The size of the water droplet was determined from the image taken with the high-speed camera.

## III. RESULTS AND DISCUSSION

### A. V-I Characteristic

Figures 2 show the voltage-current (V-I) characteristics in the electro spray with the 0.3 mm nozzle. The V-I was measured with the syringe filled with deionized water. The current started to increase at about 6 kV, which is assume to be the corona onset voltage. As the applied voltage further increased, the current exhibited a rapid exponential growth. The current value reached to 14.5  $\mu$ A at 17 kV. Within the tested applied voltage a stable current waveform without any current pulses were observed, which is belong to a typical Hermstein's glow discharge. [17].

Since the measured current is the sum of charge carried by electrically charged water droplets and the gas ions produced by corona discharge as well, it is difficult to measure the net charge carried by the droplets in the presence of corona discharge.

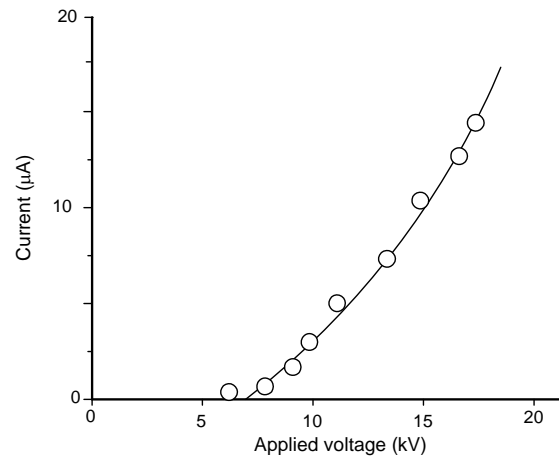


Fig.2 Voltage-Current characteristic of the electro spray with positive polarity (nozzle = 0.3 mm)

### B. The Influence of Applied Voltage on the Electro spray of Deionized Water

The patterns of electro spray were found to be very sensitive to the applied. Figure 3 shows the high speed camera images of the electro spray at each applied voltages. The nozzle with 0.3 mm inner diameter and 0.5 mm outer diameter was used. Magnification of each figure is not always the same, but one can estimate the scale form the size of nozzle tip. Applied voltage was found to be an important factor affecting the spray pattern. The spray was observed below the corona onset voltage. A dripping mode appeared at around 5.2 kV. At 5.4 kV, a mixed mode of dripping and jet emitting was observed. The dripping mode changed into spindle mode at 6.0 kV. The length of water filament in the spindle mode increased with the applied voltage. The spindle mode consisted of several stages (extension of water filament from the meniscus, fine jet emission, detachment of the water filament form the nozzle, break-up of filament) and repeated in the same order. The repetition frequency of each spindle event was also increased with the applied voltage; 200 Hz (6 kV), 300 Hz (7.2 kV), 380 Hz (8.2 kV) and 280 Hz (9 kV). On the other hand, the length of the water filament just before detaching from the nozzle exhibited a linear increase with the applied voltage; 2.5 mm (6 kV), 3.2 mm (7.2 kV), 3.9 mm (8.2 kV) and 5 mm (9 kV).

The spray pattern greatly changed at voltage higher than 10 kV. The filament started to oscillate periodically from side to side. As the applied voltage further increased above 12 kV, the water filament started to rotate. The tip of the filament swirled vigorously and this swirl movement produced fine droplets. Except for the swirl movement at the filament front, the circular movement of filament stopped at 14 kV, and resulted in a stable cone-jet with a long filament (about 3.7 mm). The further increase of the applied voltage extended the length of the filament up to 10 mm, whereas the spray pattern became random and unstable. Borra *et al* also reported a similar influence of applied voltage on the modes of electro spray for ethanol and water [18]. They also indicated that corona discharge plays an important role in changing the spray pattern. Jaworek and Krupa have studied the corona discharge in

5.4 kV	6 kV	8.2 kV		10kV	12 kV	14 kV	16 kV
Dripping with jet	Spindle	Spindle		Oscillating cone-jet	Rotating cone-jet	Stable Cone-jet	Unstable cone-jet
							
							

Figure 3. High speed camera images of the electrospray of deionized water (0.5 mm nozzle, positive DC).

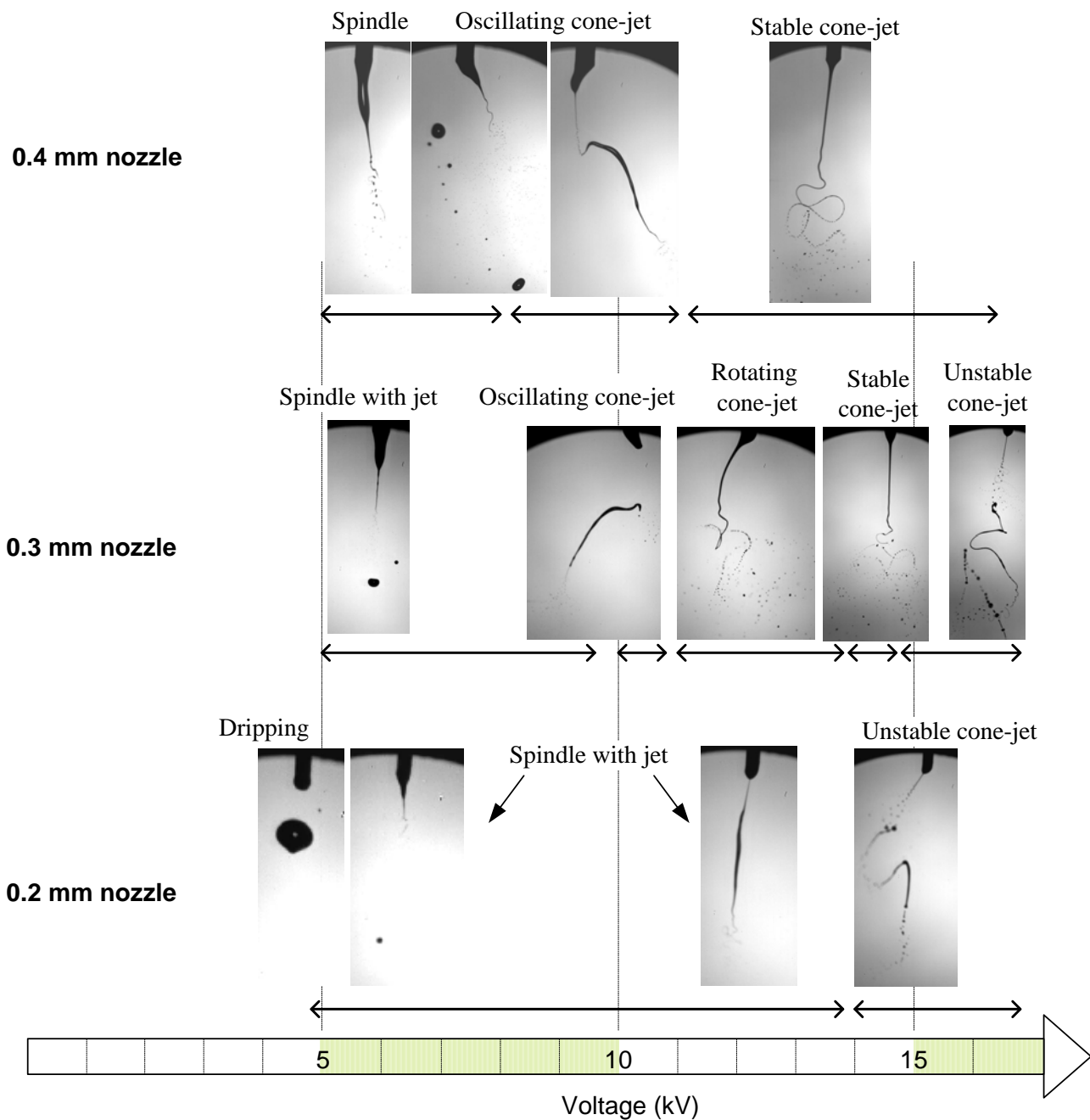


Figure 4. The influence of nozzle diameter on the mode of electrostatic spray.

electrohydrodynamic (EHD) spraying and found that the region of corona discharge is highly correlated to the spray pattern [19].

The size of droplet seemed to be determined mostly by the spray pattern rather than the applied voltage. Regardless of the voltage conditions, fine droplets mostly formed at the tip of the jet. The break-up of the jet or the water filament produced droplets with relatively wide size range from several tens micrometer to several 100s  $\mu\text{m}$ . At applied voltage below 5.2 kV, droplets with a diameter larger than that of the needle tip form, break off and fall away. As dripping mode starts, the

water started to protrude from the needle with a smaller diameter than the needle. The size of the droplets produced at the tip of the fine filament ranged below about 15  $\mu\text{m}$ . The break-up of long filament-like jet produced relatively large droplets between 100 – 200  $\mu\text{m}$ . The rotating and stable cone-jet with long filament produced bimodal size distribution one at 10-20  $\mu\text{m}$  and the other at 60-80  $\mu\text{m}$ . It is interesting to note that the swirl of the filament extended from the cone-jet is the main driving force to generate relatively uniform fine droplets. This is more or less close to a mechanical force rather than an electrostatic force. As the cone-jet became unstable at

16 kV, the size distribution of water droplet also became poor form several micrometer to several hundreds micrometers.

### C. The Effect of Nozzle Diameter

Figure 4 illustrates the effect of nozzle diameter on the electro-spray pattern. In the case of 0.3 mm nozzle, as shown in Figure 3, the stable cone-jet mode with a long filament only appeared at 14.0 kV. This stable cone-jet with long filament could not observe with the 0.2 mm nozzle. On the other hand, the stable cone-jet existed over relatively wide voltage range from 12.4 kV to 16.3 kV with the 0.4 mm nozzle. This stable cone-jet mode with long filament in an electro-spray of deionized water has been also reported by Jaworek and Krupa [19]. Multi-jet was not observed at the tested conditions in this study.

It should be also noticed that the increasing applied voltage promote the liquid flow rate through the nozzle. A quantitative analysis on the voltage effect on the volumetric flow rate has been reported by Smith et al in 2006 [20]. This relationship is also important in considering the scaling law based on the liquid flow rate, current and the droplet size [21-23]. The mechanism behind the electro-spray and the applied voltage (or, the presence of corona discharge) is still not well understand and requires further investigation.

## IV. CONCLUSION

A high speed camera was used to observe fine structure of the positive electro-spray of deionized water. The main findings in this study can be summarized as follows.

- 1) Spray mode were changed with from dripping mode, spindle, oscillating cone-jet, rotating cone-jet and stable cone-jet with long filament as voltage increase.
- 2) The size of droplet seemed to be determined mostly by the spray pattern rather than the applied voltage. Regardless of the voltage conditions, fine droplets mostly formed at the tip of the jet. The break-up of the jet or the filament produced wide size range up to several hundreds  $\mu\text{m}$ . The rotating and stable cone-jet with long filament produced bimodal size distribution one at 10-20  $\mu\text{m}$  and the other at 60-80  $\mu\text{m}$ .
- 3) Nozzle diameter was also found to be an important parameter determining the spray pattern. The stable cone-jet mode did not appear in the case of 0.2 mm nozzle. Voltage range for the stable cone-jet with long filament mode increased with the nozzle diameter.

## REFERENCES

- [1] A. Jaworek and A. T. Sobczyk, "Electrospraying route to nanotechnology: An overview," *J. Electrostat.*, vol. 66, pp. 197-219, 2008.
- [2] J. Zeleny, "The discharge of electricity from pointed conductors," *Phys. Rev. Series*, vol. 26, pp. 129-154, 1908.
- [3] J. Zeleny, "Instability of electrified liquid surfaces," *Phys. Rev.*, vol. 10, pp. 1-8, 1917.
- [4] J. Zeleny, "Electrical discharges from pointed conductors," *Phys. Rev.*, vol. 16, pp. 102-125, 1920.
- [5] A. G. Bailey, *Electrostatic Spraying of Liquids*. New York: John Wiley & Sons Inc., 1988.
- [6] J. N. Smith, R. C. Flagan, and J. L. Beauchamp, "Droplet evaporation and discharge dynamics in electro-spray ionization," *J. Phys. Chem. A*, vol. 106, pp. 9957-9967, 2002.
- [7] K. Tang and A. Gomez, "On the structure of an electrostatic spray of monodisperse droplets," *Phys. Fluids*, vol. 67, pp. 2317-2332, 1994.
- [8] H. M. A. Elghazaly and G. S. P. Castle, "Analysis of the instability of evaporating charged liquid drops," *IEEE Trans. Ind. Applicat.*, vol. 22, pp. 892-896, 1986.
- [9] A. Doyle, D. R. Moffett, and B. Vonnegut, "Behavior of evaporating electrically charged droplets," *J. Colloid Interface Sci.*, vol. 19, pp. 136-143, 1964.
- [10] M. A. Abbas and J. Latham, "The instability of evaporating charged drops," *J. Fluid Mech.*, vol. 30, pp. 663-670, 1967.
- [11] L. D. Juan and J. F. D. L. Mora, "Charged and size distributions of electro-spray drops," *J. Colloid Interface Sci.*, vol. 186, pp. 280-293, 1997.
- [12] E. J. Davis and M. A. Bridges, "The Rayleigh limit of charged revisited: Light scattering from exploding droplets," *J. Aerosol. Sci.*, vol. 25, pp. 1179-1199, 1994.
- [13] D. Michelson, *Electrostatic Atomization*. Bristol and New York: Adam Hilger, 1990.
- [14] S. O. Shiryayeva and A. I. Grigor'ev, "The semiphenomenological classification of the modes of electrostatic dispersion of liquids," *J. Electrostat.*, vol. 34, pp. 51-59, 1995.
- [15] M. Cloupeau and B. P. Foch, "Electrostatic spraying of liquids: Main functioning modes," *J. Electrostat.*, vol. 25, pp. 165-184, 1990.
- [16] M. Cloupeau and B. Prunet-Foch, "Electrohydrodynamic spraying functioning modes: A critical review," *J. aerosol. Sci.*, vol. 25, pp. 1021-1036, 1994.
- [17] T. N. Giao and J. B. Jordan, "Modes of corona discharges in air," *IEEE Trans. Power Apparatus and Sys.*, vol. 87, pp. 1207-125, 1968.
- [18] J. P. Borra, Y. Tombette, and P. Ehouam, "Influence of electric field profile and polarity on the mode of EHDA related to electric discharge regimes," *J. Aerosol. Sci.*, vol. 30, pp. 913-925, 1999.
- [19] A. Jaworek and A. Krupa, "Classification of the modes of EHD spraying," *J. Aerosol. Sci.*, vol. 30, pp. 873-893, 1999.
- [20] K. L. Smith, M. S. Alexander, and J. P. W. Stark, "Voltage effects on the volumetric flow rate in cone-jet mode electro-spraying," *J. Appl. Phys.*, vol. 99, p. 064909, 2006.
- [21] J. M. Lopez-Herrera, A. Barrero, A. Lopez, I. G. Loscertales, and M. Marquez, "Coaxial jets generated from electric Taylor cones. Scaling laws," *J. Aerosol. Sci.*, vol. 34, pp. 535-552, 2003.
- [22] A. M. G. Calvo, J. Davila, and A. Barrero, "Current and droplet size in the electro-spraying of liquids. Scaling laws," *J. Aerosol. Sci.*, vol. 28, pp. 249-275, 1997.
- [23] A. M. Gañán-Calvo, "Cone-jet analytical extension of Taylor's electrostatic solution and the asymptotic universal scaling laws in electro-spraying," *Phys. Rev. Lett.*, vol. 79, pp. 217-220, 1997.